Shock Waves (2001) 11: 199–207

Shock Waves

Transition between regular and Mach reflection of shock waves: new numerical and experimental results

M.S. Ivanov[1], D. Vandromme[2], V.M. Fomin[1], A.N. Kudryavtsev[1,2], A. Hadjadj[2], D.V. Khotyanovsky[1]

[1] Institute of Theoretical and Applied Mechanics, 630090 Novosibirsk, Russia
[2] LMFN-CORIA, INSA de Rouen, 76801 St. Etienne du Rouvray, France

Received 23 November 2000 / Accepted 25 April 2001

Abstract. New numerical and experimental results on the transition between regular and Mach reflections of steady shock waves are presented. The influence of flow three-dimensionality on transition between steady regular and Mach reflection has been studied in detail both numerically and experimentally. Characteristic features of 3D shock wave configuration, such as peripheral Mach reflection, non-monotonous Mach stem variation in transverse direction, the existence of combined Mach-regular-peripheral Mach shock wave configuration, have been found in the numerical simulations. The application of laser sheet imaging technique in streamwise direction allowed us to confirm all the details of shock wave configuration in the experiments. Close agreement of the numerical and experimental data on Mach stem heights is shown.

Key words: Steady shock waves, Regular reflection, Mach reflection, Transition criteria, Hysteresis phenomenon, 3D effects

1 Introduction

The transition between regular and Mach shock wave reflections, having more than a century's history of research, still remains one of the last unsolved problems of classical gas dynamics. The existence of two possible solutions at the same flow conditions, and related hysteresis phenomenon make this problem be one of the most interesting and challenging research tasks.

We consider here a case when a steady incident shock wave generated by a wedge reflects from a plane of symmetry (the plane of symmetry replaces a reflecting wall in order to eliminate boundary layer effects). In this case two reflection types are possible, regular and Mach reflection (see, for example, Hornung 1986, Ben-Dor 1991). In the first case (Fig. 1a), a reflected shock wave, RS, is formed at the intersection point of the incident shock, IS, and the symmetry plane. The flow that passes through the RS returns to its original direction parallel to the oncoming flow. For the Mach reflection (Fig. 1b), the point T where the incident and reflected shocks intersect, is located at some distance from the symmetry plane and is bridged with it by the third shock wave, Mach stem MS. Besides three shock waves, a slip surface, SS, also emanates from the triple point T and separates the streams passed through the MS and through two shocks, IS and RS. The existence of Mach reflection in steady flow is connected with the presence of the length scale (the wedge length w) that determines the Mach stem height H_{st}. The trailing edge of a wedge generates an expansion fan that is refracted on the RS and then interacts with the SS. Due to this interaction, the slip surface becomes curved and forms "a virtual nozzle" (Hornung and Robinson 1982). In this nozzle the subsonic flow behind the Mach stem accelerates up to a supersonic velocity. The Mach stem height is defined by the relation between the inlet and throat cross-sectional areas of the virtual nozzle.

The transition from one reflection type to the other at a fixed free stream Mach number occurs at a certain incident shock angle α_{tr}. The analysis of two-shock and three-shock configurations made by von Neumann in his classical work (von Neumann 1943) allowed to derive two principal criteria for strong shock waves (M > 2.2) – the von Neumann (or mechanical equilibrium) criterion, α_N, and the detachment criterion, α_D, at which the transition from regular to Mach reflection may occur. Regular reflection is impossible for $\alpha > \alpha_D$, and Mach reflection is impossible for $\alpha < \alpha_N$. In the range $\alpha_N \le \alpha \le \alpha_D$ (dual solution domain) both reflection types are theoretically possible. The difference $(\alpha_D - \alpha_N)$ increases considerably when increasing M. For example, it reaches 8.5° for M = 5 (see Fig. 2).

Theoretical possibility of the existence of two different shock configurations for $\alpha_N \le \alpha \le \alpha_D$ implies a question: which criterion is correct for the transition between these configurations? Unfortunately, up to now, there is no definite answer to this simple question. In this paper we present new experimental and theoretical findings on

Correspondence to: A.N. Kudryavtsev
(e-mail: alex@itam.nsc.ru)

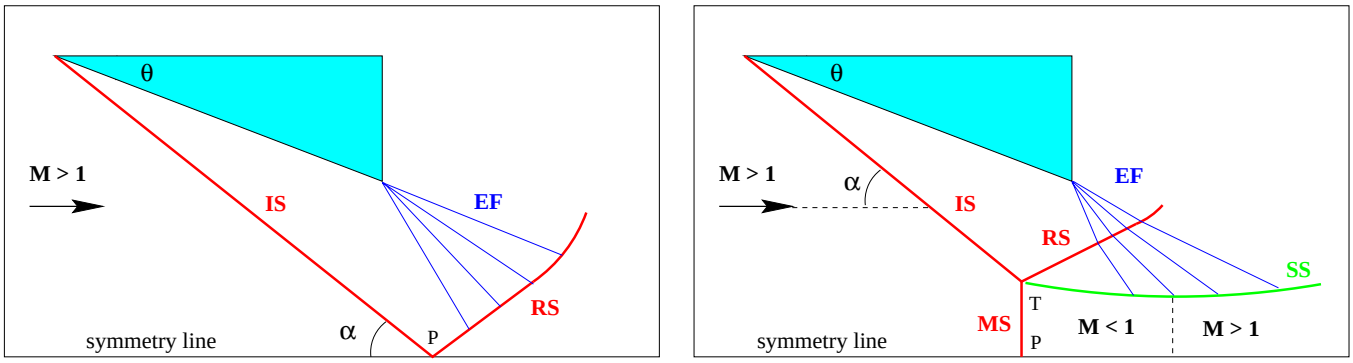

Fig. 1. The schematic of the flow at regular **a** and Mach **b** reflection

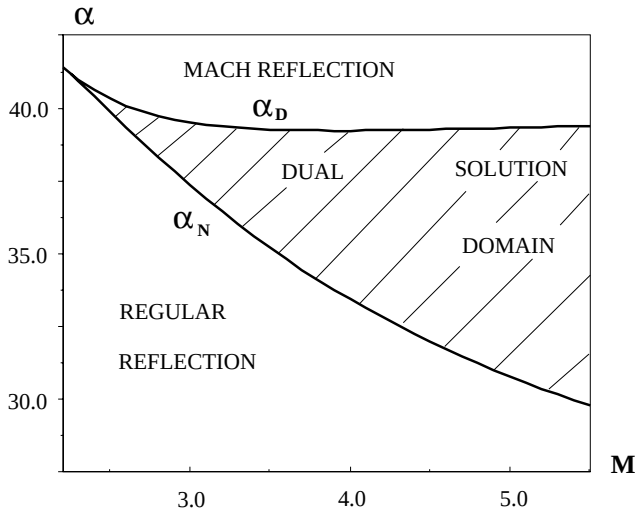

Fig. 2. The dual solution domain

the shock wave reflection transition resulted from a joint research project[1].

The next section briefly reviews state-of-the-knowledge of the problem of transition between regular and Mach reflections in steady flows. Section 3 describes in details the most important new experimental and numerical results obtained in the course of the project completion.

2 Previous studies

The hypothesis that a hysteresis phenomenon may exist in the transition between regular (RR) and Mach (MR) reflections of strong shock waves in steady flows was first put forward by Hornung et al. (1979). It was assumed that when the angle of incidence, α, changes continuously, the transition from RR to MR and the reverse transition occur at different α values, that is $\alpha_{\mathrm{RR}\to\mathrm{MR}}$ transition is at α_D and reverse $\alpha_{\mathrm{MR}\to\mathrm{RR}}$ transition is at α_N. An attempt to confirm this hypothesis was performed experimentally by Hornung and Robinson (1982) and gave a negative result: no hysteresis was observed, that is both transitions occurred at the angles close to von Neumann criterion. It was concluded by Hornung and Robinson (1982), that a possible reason might be the disturbances inherent in wind tunnel flow, which could affect the transition. However, the hysteresis was later obtained experimentally by Chpoun et al. (1995), and numerically by Ivanov et al. (1995) using the Direct Simulation Monte Carlo (DSMC) method. In more recent studies of Ivanov et al. (1996a), Hadjadj et al (1997), Ivanov et al. (1998a) the hysteresis phenomenon was examined carefully using two numerical approaches, kinetic and continuum. These numerical studies proved the existence of the hysteresis in accordance with the prediction of Hornung et al. (1979). In Fig. 3 the results of Euler computations at M = 4 for the same incident shock angle α are given. The theoretical criteria for this Mach number are $\alpha_N = 33.44$, $\alpha_D = 39.23$. First, the RR was numerically obtained for $\alpha < \alpha_N$. When α was increased within the dual solution domain the RR persisted, then at α slightly above α_D the RR $\to$ MR transition occured, and then when α was decreased the MR configuration persisted in the flow.

Cited above experiments of Chpoun et al. (1995) gave a clear evidence of hysteresis, but some details of these experiments, such as the angle of transition from RR to MR, α_{tr}, do not correspond to what comes from the hypothesis of Hornung et al. (1979) (α_{tr} was 37.2° instead of $\alpha_D = 39.3°$ for M = 4.96). This was probably caused by three-dimensional effects which were significant in these experiments where a wedge model with a small spanwise size was used. The contradiction motivated conducting new experiments by Ivanov et al. (1997) where different aspect ratios, i.e. ratios of the wedge span to its length, were used, from 0.66 up to 3.75. The existence of hysteresis was confirmed there, but the total agreement of experimental and numerical data was not obtained.

The reasons for the discrepancies between experimental and numerical transition angles and for those existing between the results obtained at different experimental facilities are supposed to be twofold. The first rea-

[1] The project (coordinated by Prof. Dany Vandromme) included five scientific teams from Russia, France and Belgium and was supported by INTAS (International Association for the promotion of cooperation with scientists from the New Independent States of the former Soviet Union).

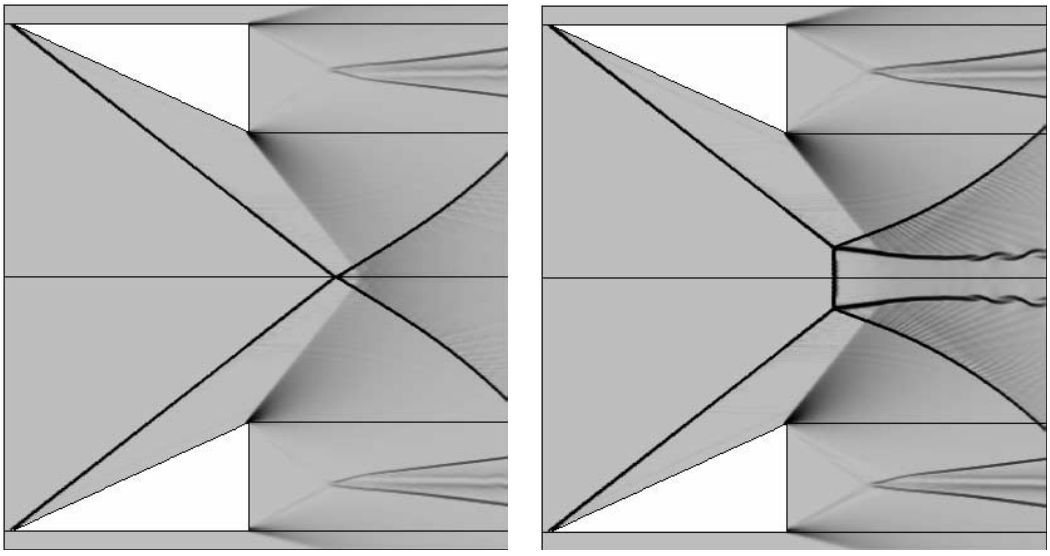

Fig. 3. Regular (*left*) and Mach (*right*) reflections at M = 4 and the same incident shock angle $\alpha = 38^\circ$. Euler computations

son is the effect of the free stream disturbances, which must be accounted for when considering conditions of the transition in the wind tunnels. The effect of the disturbances was investigated numerically (Ivanov et al. 1998a, Khotyanovsky et al. 1999). It was shown that the perturbations of some kind can indeed lead to a "stimulated" transition between the two types of reflection. It was also found that RR $\rightarrow$ MR transition can be achieved easier than the reverse transition, and the levels of the perturbation, necessary for this transition, decrease when approaching to the upper limit of the existence of RR, α_D. Still, the amplitudes of these disturbances can hardly be relevant to the real experimental flows, and it is not clear why the RR $\rightarrow$ MR transition in some experiments takes place near α_N.

The other reason for the discrepancies is the flow three-dimensionality, which is also present in the experiments where the wedges of finite span are used as the test models. These effects are now being extensively studied in detail, both numerically and experimentally. Detailed theoretical consideration of these was provided by Skews (1997). Depending on the wedge relative span b/w the shock wave configuration may either have a 2D portion in the vertical plane of symmetry, or the overall configuration may be purely three-dimensional when the rarefaction waves from the wedge tips reach the inner portion of the flow. Three-dimensionality is even more cruicial for the Mach reflection when a subsonic region behind the Mach stem surface exists, and the rarefaction can affect the inner flow through this region. In other words, Mach reflection is *always* three-dimensional. In previous numerical studies (see, for example, Ivanov et al. 1998a) it was shown that three-dimensionality may affect the transition between RR and MR: the angles of the transition increase when b/w decreases. The transition angles correspond to two-dimensional criteria only for sufficiently high aspect ratios b/w, say $b/w > 4$. It was also confirmed numerically (Ivanov et al., 1998a) that a hysteresis phenomenon in RR $\leftrightarrow$ MR transition exists in 3D case too.

In the following we will discuss the most recent numerical and experimental results on the transition between regular and Mach reflection. The investigation of the effects of flow three-dimensionality is of primary interest in this paper.

3 Present study

3.1 Numerical techniques

Numerical modelling can provide a great amount of information concerning the 3D structure of shock wave reflection and be a most useful tool for its investigation. Such numerical studies were started by Ivanov et al. (1996b), Ivanov et al. (1998a). In those studies the 3D shock wave structure was investigated with DSMC (Direct Simulation Monte-Carlo) method and also using Euler approach. In this paper we will present the results obtained with Euler computations.

The flow around two symmetrical bodies used as shock wave generators is investigated – see Fig. 4, where necessary notions are also given. This double wedge configuration is exactly the same as that experimentally studied in a number of works devoted to transition between RR and MR, and was used in DSMC computations of Ivanov et al. (1996b), Ivanov et al. (1998a). In the Euler computations, the wedges are replaced by two inclined flat plates for easier body-fitted grid generation. There is no essential difference between the results obtained with wedges or plates.

Owing to the symmetry of the problem, the computations have been performed only in a quarter of the domain. The downstream boundary is located far enough so that the flow there was supersonic. The upper and

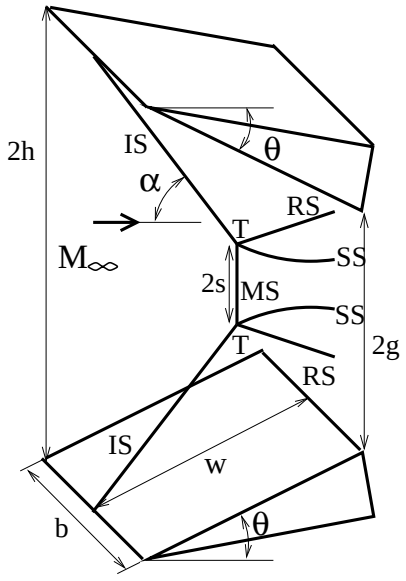

Fig. 4. Schematic of the double-wedge configuration

lateral boundaries are chosen sufficiently far from the body so that a uniform free stream flow could be prescribed on them. The angle of the wedge-generated oblique shock wave is changed by rotating the wedge around its trailing edge, so that the distance g between the horizontal symmetry plane and the trailing edge is constant during the rotation.

The three-dimensional unsteady Euler equations for perfect gas (the specific heats ratio $\gamma = 1.4$) are solved with a high-order total variation diminishing (TVD) scheme.

The HLLE (Harten-Lax-van Leer-Einfeldt) solver is used to calculate the numerical fluxes on the inter-cell boundaries because of its robustness for flows with strong shock waves and expansions. The variables in the "left" and "right" states on the inter-cell boundaries are reconstructed from cell averaged ones using the 4-th order formula of Yamamoto and Daiguji (1993). The reconstruction is applied to the primitive variables (density, velocity components and pressure). The use of a high-order reconstruction formula allows us to decrease a large numerical diffusion inherent to the HLLE solver and provide a high resolution of the smooth part of the solution without the loss of robustness near strong shock waves. The third-order explicit TVD Runge-Kutta scheme is chosen as a time stepping method. It should be noted that an accurate modelling of unsteady phenomena can prove to be important in this problem. A multi-block body-fitted grid is used in simulations with the number of cells up to 945,000. For a more detailed description of the numerical method, see Ivanov et al. (1998b).

3.2 Wind tunnel facility and experimental set-up

New experiments aimed at investigating the effects of three-dimensionality have been performed in the wind tunnel T-313 of the Institute of Theoretical and Applied Mechanics (ITAM) at the Mach number M = 4. This wind tunnel has a rectangular closed test section of 600 mm × 600 mm size. The stagnation temperature of air was equal to 290° C and the pressure in the settling chamber was 10 atm. Two symmetrical wedges with the length $w = 80$ mm mounted in the wind tunnel test section were used as shock wave generators.

The angle of attack θ and, consequently, the angle of generated shock wave α can be varied by simultaneous rotation of the wedges around their trailing edges. Thus, the distance between the trailing edges, $2g$, remains constant during rotation. Models with a different spanwise width b were used to consider the shock wave reflection with more or less three-dimensional effects.

The investigation of 3D structure of flow is a challenging task for the experimental research. Common schlieren visualization, which is widely used in experiments, produces flow images integrated along the spanwise direction, see Fig. 5 where experimental schlieren for the Mach reflection is given. For comparison, the "numerical schlieren", that is density gradient integrated along transverse coordinate, is also given. It is not easy to extract the information on 3D shock wave configuration from these integrated images. An oblique shadowgraphy technique with the inclined optical axis was utilized by Skews (2000) for this problem and some valuable features of the flow could then be deduced from these visualizations.

More detailed information can be provided by use of laser sheet imaging technique (vapor screen visualization). This technique utilizes the laser light scattering on micron-sized particles of water. As a result, only the flow in the plane of the laser sheet is visualized, in contrast to the common schlieren technique. The spanwise laser sheet visualization was employed by Sudani et al. (1999) to investigate the structure of 3D shock wave reflection, and gave some promising results. In our study we developed similar technique with the laser sheet in streamwise direction. A schematic of experimental set-up and optical diagnostic system is shown in Fig. 6.

As a light source, an argon-ion laser was used. The power of the laser was adjusted at 3 W to provide clear pictures.

The laser beam was expanded to a light sheet 1 mm thick by means of a combination of convex and spherical lenses. The laser sheet was introduced into the flow using a small prism mounted on a side wall in the subsonic part of the wind tunnel, approximately 1 m upstream of the nozzle throat and 4.5 m upstream of the test section. It causes only a small distortion of the surrounding low-speed stream and has no influence on the supersonic flow in the test section.

In order to investigate the 3D structure of shock wave reflection configurations, the laser sheet was traversed in the spanwise direction scanning the flowfield from the central plane of the test section up to the wall. The maximum angle between the laser sheet and the wind tunnel axis did not exceed 3.8°. An appropriate amount of water (less than 1.1 g_{H_2O}/kg_{air}) was seeded in the wind tunnel be-

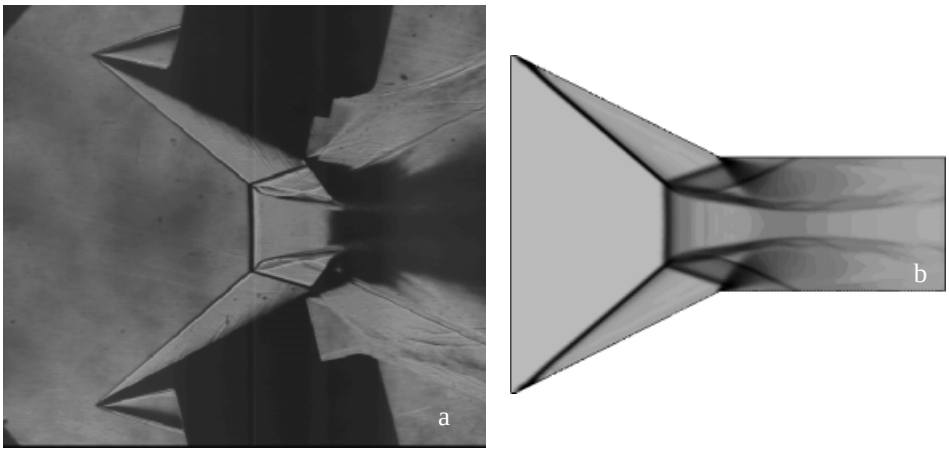

Fig. 5. Experimental schlieren **a** and "numerical schlieren" **b** for the MR at the same flow conditions

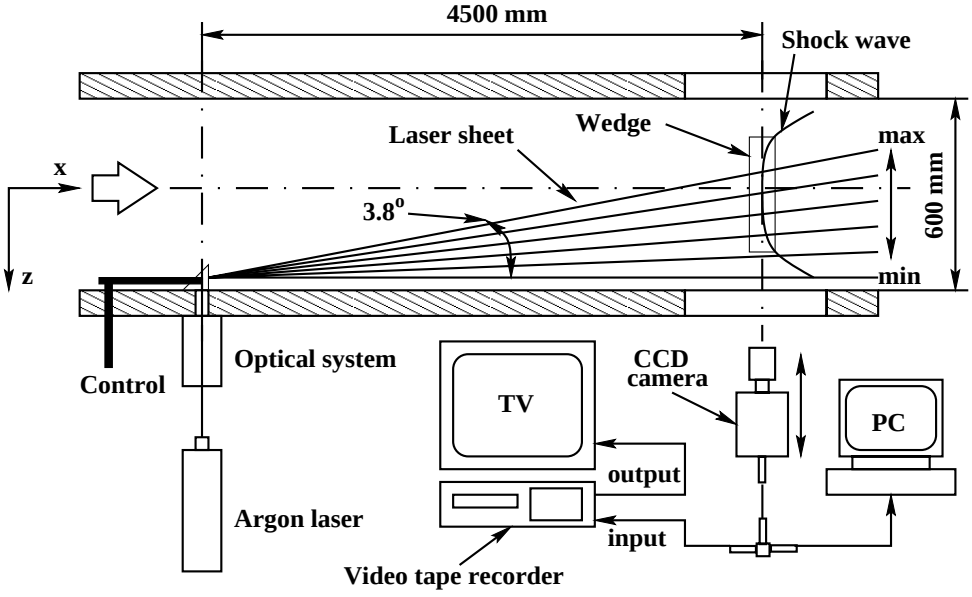

Fig. 6. Schematic of experimental set-up (*top view*) and optical diagnostic system

fore the settling chamber. Slices of the flow pattern were grabbed by the CCD camera mounted outside the test section. To avoid the image scale disturbances the movement of the CCD camera was synchronized with the laser sheet movement. The maximum number of flow images corresponding to different streamwise planes, which were obtained at different spanwise locations during one pass across the test section, was equal to 20. The CCD camera was connected to both the computer frame grabber and the video tape recorder (VTR).

3.3 Results

Normalized Mach stem heights s/w obtained numerically are shown in Fig. 7 vs. the shock wave angle α. For comparison, the experimental values for the corresponding flow conditions are also given. The free-stream Mach number is here equal to M = 4 (for this M, $\alpha_N = 33.4°$ and $\alpha_D = 39.2°$). The transition to MR occurred when α was increasing from 39° to 40°. When the shock wave angle was decreasing, MR was preserved down to 36°, and RR was formed at $\alpha = 35°$. Thus, the results of simulations give clear evidence that, within the dual solution domain, the final reflection type depends on initial conditions and the hysteresis exists as well as in 2D numerical simulations. Moreover, the transition angles are in reasonable agreement with the theoretical values. An earlier transition from MR to RR than in experiments can be explained by the very small Mach stem height at the angles close to α_N. This height becomes comparable with the size of numerical cells and cannot be resolved without further grid refinement. It is also clear that the numerical and experimental Mach stem heights for the same spanwise aspect ratios b/w are in beautiful agreement. Figure 7a also illustrates the influence of the wedge span on the numerical Mach stem heights (for comparison, their values at $b/w = 2$ and in 2D case are given).

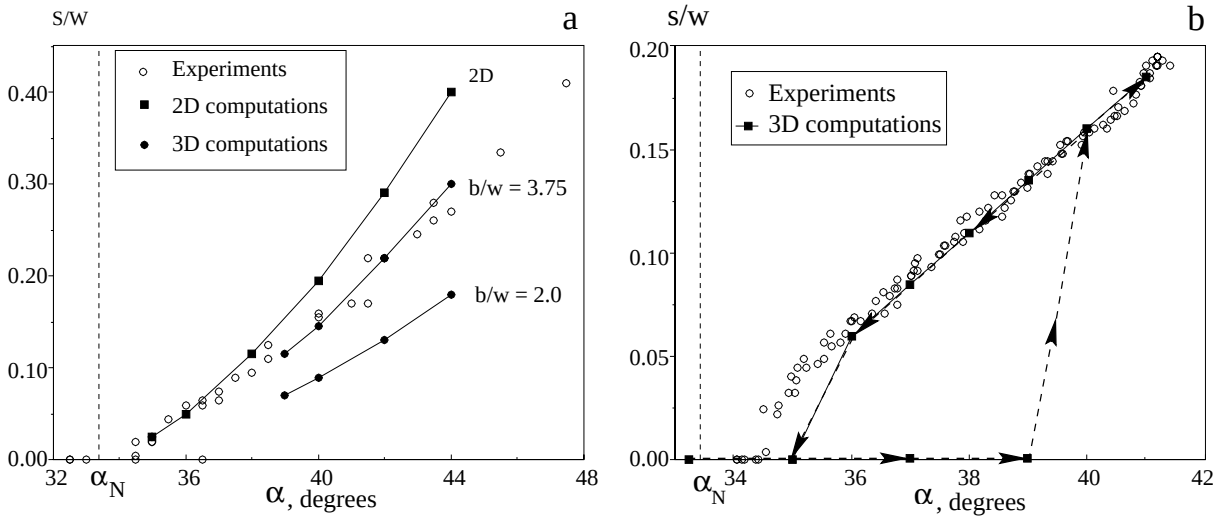

Fig. 7. Experimental and numerical Mach stem heights vs incident shock angle for M = 4; and $g/w = 0.56$, $b/w = 3.75$ **a**, and $g/w = 0.3$, $b/w = 2$ **b**

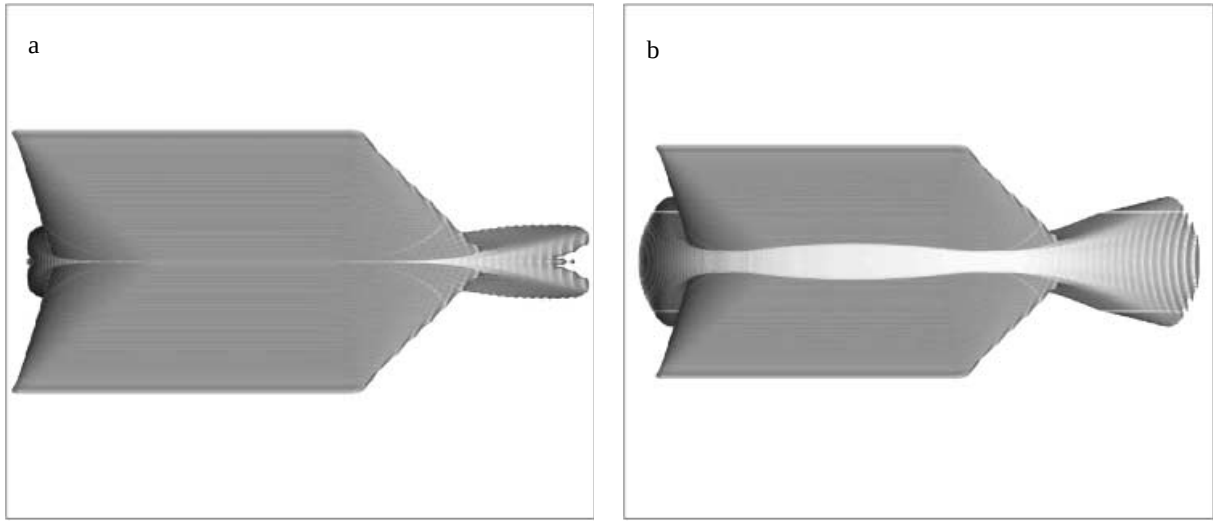

Fig. 8. Density isosurfaces $\rho/\rho_\infty = 2.2$ for RR **a** MR **b**. The Euler computations, M = 4, $\alpha = 38^\circ$, $b/w = 2$, $g/w = 0.3$

Numerical modelling allows us to reconstruct 3D shapes of shock waves generated by the test model. Figure 8 shows these shapes for RR and MR obtained by visualizing the density isosurfaces with a proper density value. They are computed for the same angle of incidence $\alpha = 38^\circ$ within the dual solution domain. An important feature of RR configuration is the existence of a peripheral Mach reflection with a supersonic flow behind the Mach stem surface. There is a point where the RR and peripheral MR co-exist in equilibrium. The most prominent feature of 3D Mach reflection is a non-monotonous behaviour of the Mach stem height in the transverse direction: its height has a maximum in the vertical plane of symmetry, closer to periphery its height decreases, reaches a minimum, and then increases again forming a peripheral Mach reflection similar to that observed in RR case.

More detailed information can be derived from two-dimensional slices of the flowfield at different values of the spanwise coordinate z ($z = 0$ refers to the vertical plane of symmetry). These are shown in Fig. 9 for RR and MR. It can be noted that at large z (on the periphery) the Mach stem is convex to the approaching flow. Far from the test model, both the incident shock and Mach stem degenerate into a weak conical wave.

All these features of 3D shock wave reflection configuration, first obtained numerically, have been confirmed in our recent experiments. Figure 10 presents laser sheet visualizations taken at different spanwise locations of the laser sheet for overall RR and MR configurations, respectively. Comparing these laser images with the results of 3D computations in Fig. 9 it is clear that all the features obtained in the numerical simulation are present in the

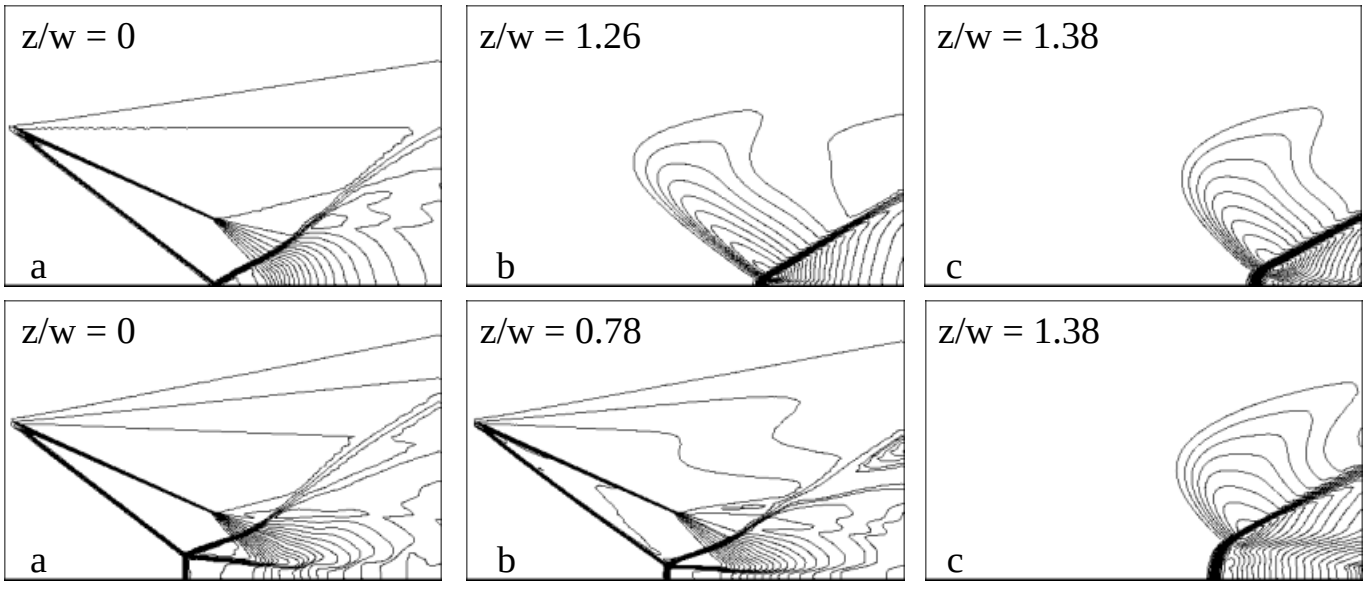

Fig. 9. Two-dimensional slices of density for RR (*top*) and MR (*bottom*). The Euler computations, M = 4, $\alpha = 38°$, $b/w = 2$, $g/w = 0.3$

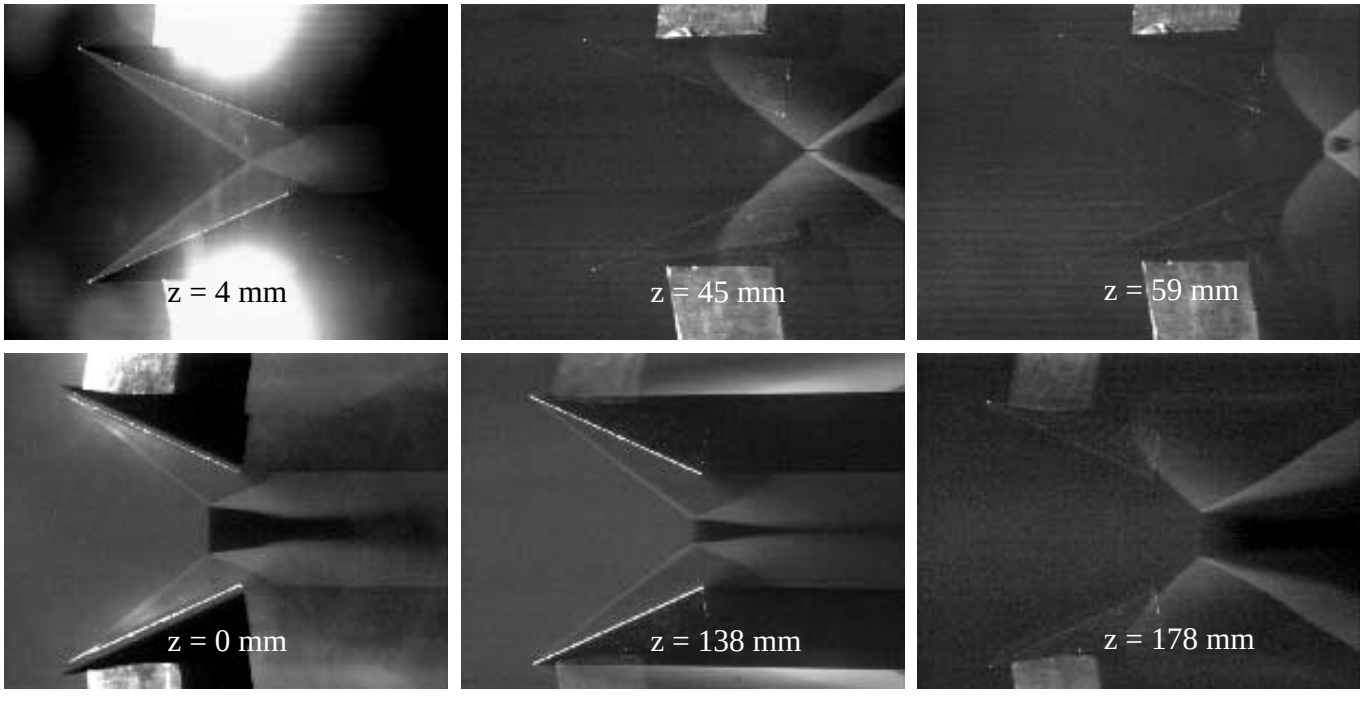

Fig. 10. Laser-sheet images for RR (*top*, $\alpha = 35°$, $b/w = 0.66$, $g/w = 0.15$) and MR (*bottom*, $\alpha = 37°$, $b/w = 3.75$, $g/w = 0.3$) at three spanwise positions at M = 4

experiments: peripheral Mach reflection, even for overall regular reflection; non-monotonous Mach stem height in case of Mach reflection.

If the Mach stem height in the central plane is small enough, then a particular shock wave configuration with a combined type of reflection is possible: MR with a small stem in the central plane, RR at some spanwise distance to the periphery, and MR again – even farther to periphery. This configuration was revealed with DSMC method Ivanov et al. (1998b), and now its existence has been confirmed with Euler computations, and is shown in Fig. 11.

This shock reflection configuration, first observed numerically, has been recently identified in our experiments. Series of images in Fig. 12 shows the Mach reflection at $z = 0$ mm, then regular reflection at $z = 158$ mm, and peripheral Mach reflection at large distance from the central plane $z = 198$ mm.

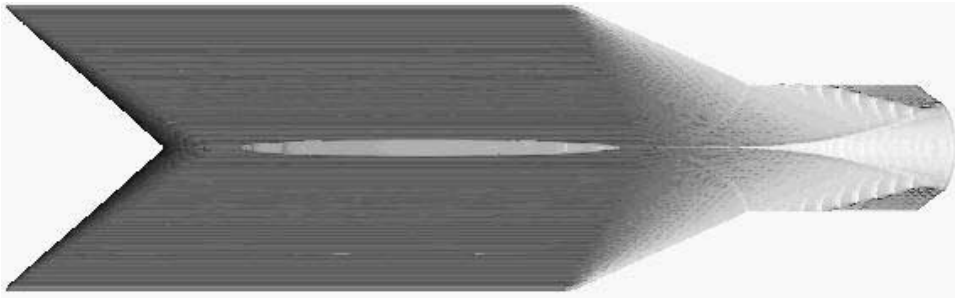

Fig. 11. Combined type of shock wave reflection. $\alpha = 35.5°$, $b/w = 3.75$, $g/w = 0.3$. Euler computations

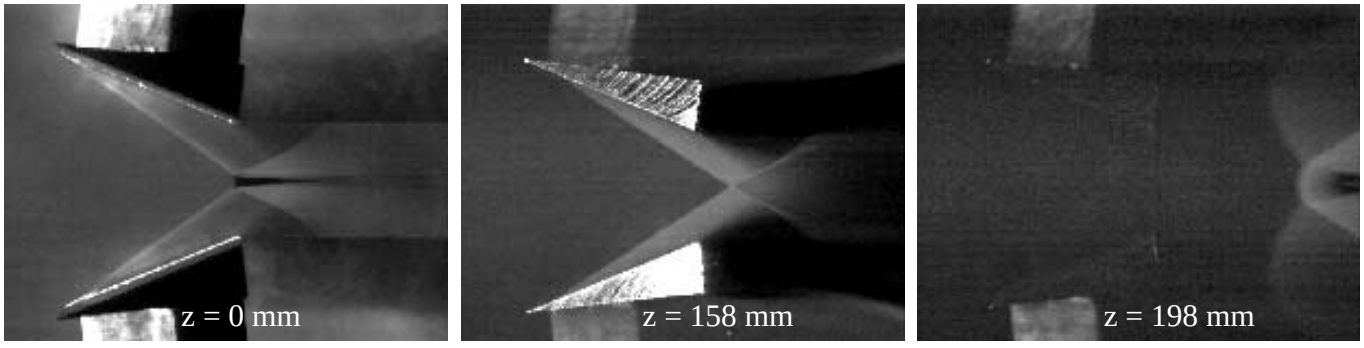

Fig. 12. Combined type of shock wave reflection. Laser sheet images at three spanwise positions. $\alpha = 34°$, $b/w = 3.75$, $g/w = 0.3$

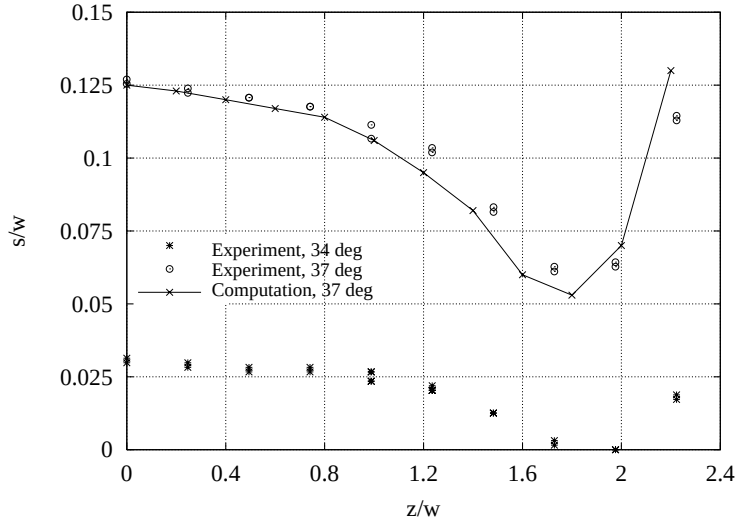

Fig. 13. Mach stem height variation in spanwise direction. M = 4, $b/w = 3.75$

The experimental laser sheet visualizations allow us to measure the Mach stem heights variation along the spanwise coordinate, which is shown in Fig. 13 for two incident shock angles α. These correspond to shock wave configurations of overall Mach reflection at $\alpha = 37°$ and intermittent reflection at $\alpha = 34°$. For comparison, the Mach stem heights obtained in our 3D Euler computations for the incident shock angle $\alpha = 37°$ are also given. It is quite evident, that experimental and numerical data are in close agreement.

4 Conclusions

Three-dimensional regular and Mach reflections of steady shock waves are studied both numerically and experimentally. The hysteresis phenomenon during the transition between two types of reflection has been observed in the numerical computations. In experiments both transitions from regular to Mach reflection, and back, take place near the von Neumann angle.

A three-dimensional shock wave configuration has been studied in detail. Peripheral Mach reflection; nonmonotonous Mach stem evolution in spanwise direction; and a combined reflection configuration with Mach reflection in the inner portion of the flow, regular reflection at some distance in spanwise direction, and peripheral Mach reflection at far periphery have been numerically shown to exist.

The experiments using laser sheet visualizations confirm all the details of 3D shock wave configuration. The combined reflection is also observed in the experiments.

Acknowledgements. The support of INTAS under Joint Research Grants No. 96-2356 and No. 99-0785 and Russian Foundation for Basic Research (Grant No. 00-01-00824) is gratefully acknowledged. D. Khotyanovsky would like to acknowledge the support of INTAS Young Scientist Fellowship YSF 99-4061. We are also very thankful to all participants of the joint research projects.

References

Ben-Dor G (1991) Shock wave reflection phenomena. Springer Verlag, N.Y., USA

Chpoun A, Passerel D, Li H, Ben-Dor G (1995) Reconsideration of oblique shock wave reflections in steady flows. Part 1. Experimental investigation. J Fluid Mech 301: 19–35

Hadjadj A, Kudryavtsev AN, Ivanov MS, Vandromme D (1997) Numerical investigation of hysteresis effects and slip surface instability in the steady Mach reflection. Proc. of 21st Int. Symp. on Shock Waves (Great Keppel, Australia, 20–25 July 1997). Panther Publishing, Fyshwick, Australia 2: 841–847

Hornung HG, Oertel H, Sandeman RJ (1979) Transition to Mach reflexion of shock waves in steady and pseudosteady flow with and without relaxation. J Fluid Mech 90: 541–560

Hornung HG, Robinson ML (1982) Transition from regular to Mach reflection of shock wave. Part 2. The steady-flow criterion. J Fluid Mech 123: 155–164

Hornung HG (1986) Regular and Mach reflection of shock waves. Annual Review of Fluid Mech 180: 33–58

Ivanov MS, Gimelshein SF, Beylich AE (1995) Hysteresis effect in stationary reflection of shock waves. Phys Fluids 7(4): 685–687

Ivanov M, Zeitoun D, Vuilon J, Gimelshein S, Markelov GN (1996a) Investigation of the hysteresis phenomena in steady shock reflection using kinetic and continuum methods. Shock Waves 5(6): 341–346

Ivanov MS, Gimelshein SF, Kudryavtsev AN, Markelov GN (1996b) Numerical study of the transition from regular to Mach reflection in steady supersonic flows. International Conference on Numerical Methods in Fluid Dynamics, 394–399 (1996)

Ivanov MS, Klemenkov GP, Kudryavtsev AN, Nikiforov SB, Pavlov AA, Fomin VM, Kharitonov AM, Khotyanovsky DV, Hornung HG (1997) Experimental and numerical study of the transition between regular and Mach reflections of shock waves in steady flows. Proc. of 21st Int. Symp. on Shock Waves (Great Keppel, Australia, 20–25 July 1997). Panther Publishing, Fyshwick, Australia 2: 819–824

Ivanov MS, Markelov GN, Kudryavtsev AN, Gimelshein SF (1998a) Numerical analysis of shock wave reflection transition in steady flows. AIAA J. 36(11): 2079–2086

Ivanov MS, Gimelshein SF, Kudryavtsev AN, Markelov GN, Khotyanovsky DV (1998b) Numerical simulation of three-dimensional regular and Mach reflections of shock waves in steady flows. 4th European CFD Conference 1(2): 869–874

Khotyanovsky DV, Kudryavtsev AN, Ivanov MS (1999) Numerical study of transition between steady regular and Mach reflection caused by free-stream perturbations. Proc. of 22nd Int. Symp. on Shock Waves (London, UK, July 18–23, 1999). Imperial Colledge, London, UK, pp. 1261–1266

von Neumann J (1943) Oblique reflection of shock waves. Explosive Research Report No 12, Navy Dept. Bureau of Ordonance, Washington DC. US Dept. Comm. Off. Tech. Serv. No PB37079 (Reprinted in Collected Works of J. von Neumann, Pergamon Press, 1963, 6: 238–299

Skews BW (1997) Aspect ratio effects in wind tunnel studies of shock wave reflection transition. Shock Waves 8: 373–383

Skews BW (2000) Three-dimensional effects in wind tunnel studies of shock wave reflectiony. J Fluid Mech 407: 85–104

Sudani N, Sato M, Watanabe M, Noda J, Tate A, Karasawa T (1999) Three-dimensional effects on shock wave reflections in steady flows. AIAA Paper 99–0148

Yamamoto S, Daiguji H (1993) Higher-order-accurate upwind schemes for solving the compressible Euler and Navier-Stokes equations. Computers and Fluids 22(2/3): 259–270